



## Gigahertz spin noise spectroscopy in *n*-doped bulk GaAs

Georg M. Müller,\* Michael Römer, Jens Hübner, and Michael Oestreich

*Institut für Festkörperphysik, Leibniz Universität Hannover, Appelstraße 2, D-30167 Hannover, Germany*

(Received 4 September 2009; revised manuscript received 22 February 2010; published 31 March 2010)

We advance spin noise spectroscopy to an ultrafast tool to resolve high-frequency spin dynamics in semiconductors. The optical nondemolition experiment reveals the genuine origin of the inhomogeneous spin dephasing in *n*-doped GaAs wafers at densities at the metal-to-insulator transition. The measurements prove in conjunction with depth-resolved spin noise measurements that the broadening of the spin dephasing rate does not result from thermal fluctuations or spin-phonon interaction, as suggested previously, but from spatial *g*-factor variations.

DOI: [10.1103/PhysRevB.81.121202](https://doi.org/10.1103/PhysRevB.81.121202)

PACS number(s): 72.25.Rb, 72.70.+m, 78.47.-p, 85.75.-d

Spin noise spectroscopy (SNS) has developed into a universal tool to study the spin dynamics in quantum optics and solid-state physics. The technique utilizes the ever present spin fluctuations in electronic spin ensembles at thermal equilibrium and probes the spin-fluctuation dynamics by absorption-free Faraday rotation. First introduced by Aleksandrov and Zapasskii in a gas of sodium atoms,<sup>1</sup> the technique has been successfully transferred by Oestreich *et al.*<sup>2</sup> to semiconductor physics. This transfer is of special interest in the context of semiconductor spintronics since SNS is—in contrast to the manifold Hanle,<sup>3</sup> pump-probe Faraday rotation,<sup>4,5</sup> and time- and polarization resolved photoluminescence experiments<sup>6</sup>—a weakly perturbing technique that minimizes optical transitions from the valence to the conduction band.<sup>7</sup> SNS thereby avoids (a) heating of the carrier system which changes the spin interactions and the spin dephasing rates, (b) creation of free electrons which inevitably interact and change the spin dynamics of localized electrons, and (c) the creation of holes which drives the electron-spin dephasing by the Bir Aronov Pikus mechanism; i.e., in several cases only SNS yields the intrinsic unperturbed spin dephasing rates.<sup>8,9</sup> At the same time, SNS uniquely allows three-dimensional spatial mapping of the spin dynamics<sup>10</sup> and promises even single spin detection without destroying the spin quantum state. However, up to now these advantages could not be used to its full extent since the temporal dynamics detected by SNS has been technically limited by the available bandwidth of the detection setup. Due to the in many cases low ratio of spin noise power to background noise, efficient data averaging via analog-to-digital conversion and subsequent FFT as well as laser noise suppression via balanced photodetection is necessary. Therefore, highly sensitive SNS is technically limited by the bandwidth of commercially available digitizers and low noise balanced photoreceivers to frequencies of about 1 GHz.<sup>11</sup>

In this Rapid Communication, we demonstrate in *n*-doped GaAs—probably the most prominent model system in semiconductor spintronics—that ultrafast highly sensitive SNS (Ref. 12) becomes feasible by sampling the temporal dynamics of the electron spin with the laser repetition rate of a picosecond Ti:Sapphire laser oscillator. In the first part, we present the technique and argue that ultrafast SNS is applicable up to THz frequencies. In the second part, we combine ultrafast and depth-resolved SNS measurements<sup>10</sup> to explore the physical origin of the inhomogeneous spin dephasing in

*n*-doped GaAs close to the metal-to-insulator transition (MIT) at high magnetic fields and study the field dependence of the electron Landé *g*-factor.

Figure 1(a) schematically depicts the high-frequency SNS experimental setup. The repetition rate of an actively mode-locked ps-Ti:Sapphire laser ( $f_{\text{rep}}=80$  MHz) is doubled to  $f'_{\text{rep}}=2f_{\text{rep}}$  via a Michelson interferometerlike setup with different arm lengths. The linear polarized ps laser pulses are transmitted through an *n*-doped GaAs sample where the wavelength of the laser is tuned below the GaAs band gap to avoid absorption. The mean spin polarization of the electron ensemble in the GaAs is zero at thermal equilibrium but the root-mean-square deviation is unequal to zero and fluctuates with the transverse spin lifetime  $T_2^*$ . The spin fluctuations are mapped via Faraday rotation onto the direction of the linear polarization of the laser light which is measured by a polarization bridge. The resulting electrical signal from the balanced photoreceiver is amplified by a low noise amplifier, frequency filtered by a 70 MHz low-pass filter, seamlessly digitized in the time domain (sampling rate 180 MHz), and spectrally analyzed in real time via fast Fourier transformation. An external magnetic field *B* in Voigt geometry modulates the spin fluctuations with the Larmor precession fre-

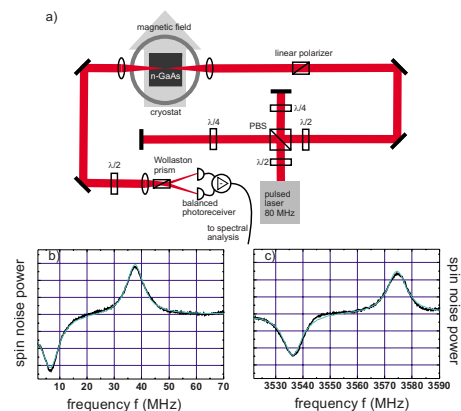


FIG. 1. (Color online) (a) Experimental setup for GHz SNS. The repetition rate of the pulsed laser is doubled via a Michelson interferometerlike setup. (b) and (c) Spin noise spectra acquired from sample A at 25 K; the peaks correspond to 6.0 and 1.0 mT (b) and to 594.7 and 588.3 mT (c), respectively. The spectra are corrected for frequency dependent amplification via division by the amplification curve. The light solid lines are Lorentzian line fits to the data.

quency  $f_L = g^* \mu_B B / h$ , where  $g^*$  is the effective electron Landé  $g$ -factor. By sampling the spin dynamics with the stroboscopic laser light, the spin noise spectrum  $S(f)$  centered around  $f_L$  evolves into a sum of noise peaks  $\Sigma_{\pm n} S(f - n f'_{\text{rep}})$ . The limit of the summation index  $n$  is given by the ratio of the inverse pulse length to the repetition rate. Due to the doubling of the original laser repetition rate, only one summand of this sum falls into the detection window. In principle, utilizing a GHz digitizer card and a fs laser system with GHz repetition rate, both commercially available, increases the bandwidth of the detection and the detectable line width to a GHz and the detectable Larmor frequencies to the THz regime. We want to point out that this sampling with pulsed laser light is not a nonlinear process such as electrical frequency mixing and thereby does not introduce any additional noise.

The two investigated samples *A* and *B* are commercial Si-doped GaAs wafers with doping densities right at the MIT ( $n_d^A = 1.8 \times 10^{16} \text{ cm}^{-3}$ ) and about four times above the MIT ( $n_d^B = 8.8 \times 10^{16} \text{ cm}^{-3}$ ) and thicknesses of 340 and 370  $\mu\text{m}$ , respectively. Both samples are antireflection coated to increase the light transmittance. The samples are mounted in a He gas flow cryostat with a superconducting split coil magnet in Voigt geometry. The magnetic field is carefully calibrated by means of a Hall probe, and the magnet system is always degaussed before starting a new series of measurement at lower magnetic fields to avoid magnetic hysteresis. The laser wavelength is set to 840 (845) nm for measurements concerning sample *A* (*B*) if not stated otherwise.

Figures 1(b) and 1(c) depict two typical spin noise spectra of sample *A* at 25 K. Electronic and optical shot noise is eliminated in these spectra by subtracting in each case two noise spectra at slightly different magnetic fields which results in a spin noise spectrum with one positive and one negative spin noise peak. The width and position of these two peaks are determined by fitting a sum of Lorentz lines to the experimental spectra. The resulting full width at half maximum of each Lorentz peak  $\Delta f_{\text{FWHM}}$  and the peak position yield the spin dephasing rate  $\Gamma_s = 1/T_2^* = \pi \Delta f_{\text{FWHM}}$  and  $g^*$ , respectively. The acquisition times of both spectra are less than 20 min. The excellent signal-to-noise ratio of the high-frequency spectrum [Fig. 1(c)] matches the signal-to-noise ratio of the low-frequency spectrum [Fig. 1(b)] proving that the ultrafast SNS comes along without loss of sensitivity.

Next, we employ high-frequency SNS and measure the transverse magnetic field dependence of  $\Gamma_s$  and  $g^*$  in bulk  $n$ -GaAs. Optical pumping techniques clearly influence both  $\Gamma_s$  (Ref. 13) and  $g^*$  (Ref. 14). We focus on the doping regime close to the MIT where an intricate interplay between localized and free electrons leads to a maximum in the low-temperature spin lifetime.<sup>15</sup> Many theoretical and experimental groups have already investigated this doping regime, but the physical origin of the experimentally observed homogeneous or inhomogeneous broadening of  $\Gamma_s$  with increasing transverse magnetic fields was up to now unsolved. Kikkawa and Awschalom, for example, measured via resonant spin amplification a plateau of the spin quality factor  $Q = g^* \mu_B B T_2^* / h$  at around 80 for a temperature of 5 K.<sup>5</sup> They attributed this maximal  $Q$ -factor—which is a measure of the

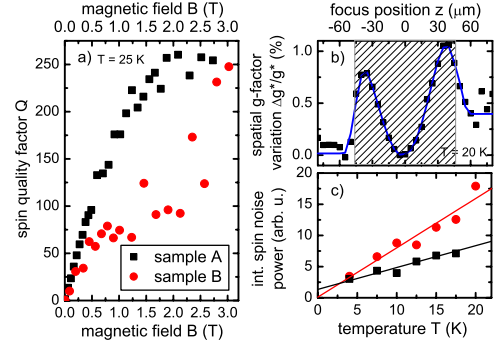


FIG. 2. (Color online) (a) Spin quality factor as a function of magnetic field. In sample *B*, the spin noise power drops for high fields which we attribute to Pauli blocking of spin noise due to filling of the Landau levels. (b) High aperture SNS measurement: shift of the electron  $g$ -factor in dependence of the position of the laser focus relative to the sample (indicated by the shaded area). The line is a guide to the eyes only. The sample appears compressed by the refractive index of GaAs. Note that the average  $g$ -factor variation with the laser focus outside the sample is lower than the average value with the focus inside. This indicates that the spin noise in the sample center contributes stronger to the GHz spin noise measurements (large Rayleigh range) than the spin noise from the sample surfaces. (c) Integrated spin noise power as a function of temperature (corrected for different sample thickness; laser wavelength: 840 nm, magnetic field: 6.75 mT). The lines are linear fits.

reduction in the spin lifetime in a transverse magnetic field—to the thermal electron distribution and the energy dependence of  $g^*$  yielding an inhomogeneous broadening. Puttika and Joynt gave a different explanation for the same experimental data and suggested a spin-phonon mechanism, which effectively leads to a homogeneous broadening of the spin dephasing rate for localized electrons.<sup>13</sup> Figure 2(a) shows the  $Q$ -factor of a similar sample (sample *A*) measured via ultrafast SNS at a lattice temperature of 25 K.<sup>16</sup> We measure a  $Q$ -factor that is, despite a five times higher temperature, about three times larger than the value reported in Ref. 5. This finding directly disproves that the  $Q$  measured by Kikkawa and Awschalom is limited by a  $g$ -factor spread resulting from a thermally broadened electron energy distribution. Such a thermally broadened  $g$ -factor spread is negligible on these time scales due to a motional narrowing type averaging in the electron energy,<sup>17</sup> which, additionally, leads to a quadratic dependence of the broadening on the magnetic field and, hence, would not result in the formation of a  $Q$ -factor plateau. The ultrafast SNS measurements also discourage the theory of thermally activated lattice vibrations since the line shape of the SNS spectrum shows a clear crossover from a homogeneously broadened Lorentzian peak to an inhomogeneously broadened Gaussian type peak.<sup>18</sup>

For further investigations of the origin of the inhomogeneous broadening, we use a high aperture cw spin noise setup (see Ref. 10 for details) in order to check for spatial electron-density variations within sample *A* that could, e.g., come from the Czochralski growth method. The unique spatial resolution strength of SNS originates from the fact that the relative noise power becomes large for small electron ensembles so that most of the SNS signal is acquired within the Rayleigh range of the laser focus. The depth-resolved

measurements are carried out in a microcryostat at a lattice temperature of 20 K, a laser wavelength of 830 nm, a Rayleigh range in vacuum of 11  $\mu\text{m}$  and accordingly a depth resolution in the sample of about 80  $\mu\text{m}$ , and a magnetic field of about 9 mT. Figure 2(b) shows the measured variation in the  $g$ -factor  $\Delta g^*/g^*$  versus focus position. The focus position is swept in this experiment from negative to positive  $z$  position where the  $z$  axis is chosen along the direction of light propagation and we define  $\Delta g^*/g^*=0$  at  $z=0$   $\mu\text{m}$ . The measurements reveal that the absolute value of  $g^*$  has a pronounced maximum close to the front and the back surface of the sample. Such a maximum of  $|g^*|$  is directly linked at this doping concentration via the energy dependence of the  $g$ -factor to a minimum in electron density.<sup>19</sup> The width of the two measured peaks is equal to the depth resolution of the laser which indicates that the spatial variation in  $g^*$  is smaller than the depth resolution of the experiment. Conductivity measurements in sample A evince hopping behavior.<sup>9</sup> This  $g$ -factor variation is not observed at higher temperatures where the conductivity significantly increases and most electrons reside in the conduction band.

We model the spatial variation in the measured  $g$ -factor by a simple phenomenological model assuming partial electron depletion at the surface, which results in a decrease in the  $g$ -factor, the spin lifetime, and the noise power at the sample surface, and get qualitative agreement with the measured SNS profile. A quantitative description is difficult due to the intricate interplay between localized and free electrons, the Fermi-level pinning, the influence of hopping and diffusion on the depletion zone, and the electric-field-induced change of  $g^*$ , the band gap, and the interband transition probability.<sup>20</sup> Nevertheless, the spatially resolved  $g^*$  variation directly entails the inhomogeneous broadening measured by ultrafast SNS where a Rayleigh range much larger than the sample thickness is employed. The much smaller  $Q$ -factor reported in Ref. 5 most likely originates from the lower conductivity at 5 K and the slightly lower doping concentration in accordance with our reasoning above. Further reasons for the observed spatial  $g$ -factor broadening could involve stress in the sample or specifics of the sample growth that we are not aware of.

Figure 2(b) shows as a second feature a spatial asymmetry of the SNS signal, i.e., the right peak is higher than the left peak and  $\Delta g^*/g^*$  is larger if the laser focus is behind the sample ( $z > 46$   $\mu\text{m}$ ) compared to the laser focus in front of the sample ( $z < -46$   $\mu\text{m}$ ). We have carefully checked that this increase does not result from a doping gradient in the sample but from the finite measurement time; i.e.,  $\Delta g^*/g^*$  increases with laboratory time and saturates after about 1 h. To account for this effect, experimental data presented in Figs. 2(a) and 3 are acquired after the saturation of this effect. We attribute this behavior to the existence of deep centers acting as an electron trap, such as the EL2 deep center, which has a metastable state with a large lattice relaxation and is excited by below band-gap excitation.<sup>21–23</sup> Such deep centers are the origin of various persistent photo effects in liquid phase grown GaAs. We exclude nuclear effects as origin since the spatial measurements were carried out at very low magnetic fields and since the integrated spin noise power also changes with time. Within the measurement error, the spin lifetime is not affected by this effect.

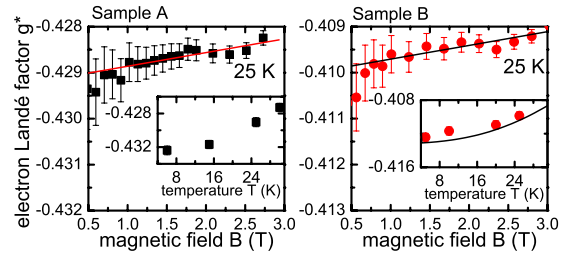


FIG. 3. (Color online) Electron Landé  $g$ -factor as a function of magnetic field for sample A and B at 25 K and as a function of the sample temperature at a magnetic field around 850 mT. The error bars of the magnetic field dependence include the inaccuracy of the magnetic field and the repetition rate  $f'_{\text{rep}}$  and the fitting errors.

Figure 2(a) also shows the  $Q$ -factor for sample B at 25 K. Within the examined field range the  $Q$ -factor does not level off as in sample A. The doping density of sample B of  $n_d^B = 8.8 \times 10^{16} \text{ cm}^{-3}$  is well above the MIT, and the electrons should therefore be delocalized. In order to directly prove the delocalized nature of the electrons in sample B, the integrated spin noise power is plotted in Fig. 2(c) for both samples as a function of temperature. The extrapolation to zero temperature yields for sample A a finite spin noise power proving partial localization of electrons. The same extrapolation yields for sample B zero spin noise power within the error bars which is consistent with delocalized electrons and Pauli blocking of the spin noise.<sup>24</sup> To our knowledge, there is no effective mechanism of inhomogeneous broadening of the spin dephasing rate for free electrons in this sample system. Hence, a strictly monotonic increase in the  $Q$ -factor with the magnetic field is expected in sample B.

Last, we study the magnetic field and temperature dependence of  $g^*$ . To our knowledge, similar investigations were only carried out for undoped or very low  $n$ -doped bulk GaAs samples.<sup>25,26</sup> Figure 3 shows the magnetic field dependence of  $g^*$  for samples A and B at 25 K. A linear fit to the magnetic field dependence of  $g^*$  between 0.5 and 3 T yields a very small magnetic field dependence of  $g_A^* = -0.4292(2) + 0.0003(1) \text{ T}^{-1} \cdot B$  for sample A and  $g_B^* = -0.4100(2) + 0.0003(1) \text{ T}^{-1} \cdot B$  for sample B at  $T=25$  K. The gradient  $dg^*/dB$  is by more than one order of magnitude smaller than for free electrons in undoped GaAs<sup>25</sup> or for donor-bound electrons at higher magnetic fields,<sup>26</sup> where  $g^*(B)$  increases in both cases by  $0.005 \text{ T}^{-1}$  due to the energy shift of the lowest Landau level which is occupied by all electrons. At the doping densities examined in this work, either Landau quantization is suppressed because of momentum scattering or several Landau cylinders are occupied since the cyclotron energy is rather low compared to the Fermi energy. The difference of  $g^*$  between the two samples extrapolated to  $B=0$  is about 0.02 which equates to a difference in Fermi energy of about 3 meV if we adapt the experimentally and theoretically reported energy dependence of  $g^*$  in GaAs of  $6.3 \text{ eV}^{-1}$  (see Ref. 19 and references therein). This difference in the Fermi energy is reasonable; i.e., the calculated difference in the Fermi level is smaller assuming only an impurity band<sup>27</sup> and larger assuming only free electrons in bulk GaAs. The same energy dependence of  $6.3 \text{ eV}^{-1}$  explains quantitatively

the absolute value and the temperature dependence of  $g^*$  for sample B. The solid line in the right inset of Fig. 3 depicts  $g^*(T)$  calculated by

$$g^*(T) = \frac{\int_0^\infty \text{DOS}(E)f(E,T)(1-f(E,T))g^*(E)dE}{\int_0^\infty \text{DOS}(E)f(E,T)(1-f(E,T))dE},$$

where  $\text{DOS}(E)$  is the three-dimensional density of states,  $f(E,T)$  is the Fermi distribution,  $g^*(E) = g_0^* + 6.3 \text{ eV}^{-1} \cdot E$ , and  $g_0^*$  is the electron Landé  $g$ -factor at the conduction-band minimum at  $T=0$  which is set to  $g_0^* = -0.481$  in agreement within the error bars of the high precession measurements of Ref. 28. The three-dimensional density of states is a good approximation for highly doped samples. For sample A, the measured temperature dependence of  $g^*$  is slightly larger than in sample B and is more difficult to calculate since donors at the MIT form an impurity band and ionization of electrons into the conduction band has to be included.

In conclusion, we have overcome the major limitation of conventional spin noise spectroscopy and demonstrated ultrafast SNS without any loss of sensitivity. We have applied the technique to  $n$ -doped GaAs at and above the metal-to-

insulator transition and proved in conjunction with depth-resolved SNS that in the sample at the MIT surface depletion changes the  $g$ -factor locally resulting in inhomogeneous spin dephasing at high magnetic fields. This mechanism is of extrinsic nature and samples at the MIT with a spatially flat Fermi level should yield significantly higher  $Q$ -factors. Measurements on the temperature dependence of the spin noise power verify the (de)localization of the electrons in the sample at (above) the MIT and ultrafast spin noise measurements yield the magnetic field and temperature dependence of  $g^*$  for thermalized electrons in the impurity and in the conduction band. Most importantly, we want to point out that ultrafast SNS is not limited to semiconductor spintronics but promises access to ultrafast spin dynamics, e.g., in atomic ensembles, magnetically ordered systems, such as ferrimagnetic garnets where recently the Bose-Einstein condensation of magnons was discovered,<sup>29</sup> or in superconductors at the phase transition.<sup>30</sup>

This work was supported by the German Science Foundation (DFG priority program 1285 “Semiconductor Spintronics”), the Federal Ministry for Education and Research (BMBF NanoQUIT), and Centre for Quantum Engineering and Space-Time Research in Hannover (QUEST). G.M.M. acknowledges support from the Evangelisches Studienwerk.

\*mueller@nano.uni-hannover.de

- <sup>1</sup>E. B. Aleksandrov and V. S. Zapasskii, *Sov. Phys. JETP* **54**, 64 (1981).
- <sup>2</sup>M. Oestreich *et al.*, *Phys. Rev. Lett.* **95**, 216603 (2005).
- <sup>3</sup>R. R. Parsons, *Phys. Rev. Lett.* **23**, 1152 (1969).
- <sup>4</sup>J. J. Baumberg *et al.*, *Phys. Rev. Lett.* **72**, 717 (1994).
- <sup>5</sup>J. M. Kikkawa and D. D. Awschalom, *Phys. Rev. Lett.* **80**, 4313 (1998).
- <sup>6</sup>A. P. Heberle, W. W. Rühle, and K. Ploog, *Phys. Rev. Lett.* **72**, 3887 (1994).
- <sup>7</sup>M. Römer, J. Hübner, and M. Oestreich, *Rev. Sci. Instrum.* **78**, 103903 (2007).
- <sup>8</sup>G. M. Müller *et al.*, *Phys. Rev. Lett.* **101**, 206601 (2008).
- <sup>9</sup>M. Römer *et al.*, *Phys. Rev. B* **81**, 075216 (2010).
- <sup>10</sup>M. Römer, J. Hübner, and M. Oestreich, *Appl. Phys. Lett.* **94**, 112105 (2009).
- <sup>11</sup>S. A. Crooker *et al.*, *Phys. Rev. Lett.* **104**, 036601 (2010).
- <sup>12</sup>S. Starosielec and D. Hägele, *Appl. Phys. Lett.* **93**, 051116 (2008).
- <sup>13</sup>W. O. Putikka and R. Joynt, *Phys. Rev. B* **70**, 113201 (2004).
- <sup>14</sup>T. Lai *et al.*, *Appl. Phys. Lett.* **91**, 062110 (2007).
- <sup>15</sup>R. I. Dzhioev *et al.*, *Phys. Rev. B* **66**, 245204 (2002).
- <sup>16</sup>The experimental values given in this Rapid Communication correspond to the most symmetric measured spin noise peaks and, hence, to the longest measured spin lifetimes since some traces show an asymmetric behavior from unknown origin. However, no systematic dependence on the angle between sample surface or magnetic field direction can be reported.
- <sup>17</sup>I. Žutić, J. Fabian, and S. D. Sarma, *Rev. Mod. Phys.* **76**, 323 (2004).
- <sup>18</sup>At moderate fields, a physical correct fit function would base upon Voigt profiles which have too many free parameters for practical purposes. Nevertheless, fitting with Gaussian profiles yields very similar peak widths as fitting Lorentzian profiles. At

- small magnetic fields and temperatures below 50 K, the temperature dependence of  $\Gamma_s$  scales with the temperature dependence of the conductivity (Ref. 9) suggesting a spin dephasing mechanism that depends on motional narrowing and should therefore be less efficient at higher  $B$  (Ref. 31).
- <sup>19</sup>M. J. Yang *et al.*, *Phys. Rev. B* **47**, 6807 (1993).
- <sup>20</sup>In our simple model, we have to assume a width of the depletion zone of some ten microns in order to mimic the measured results. A more sophisticated model would probably yield a different width. Nevertheless, we are not aware of any theoretical description of depletion zones at the MIT. Additionally, spin diffusion and electron hopping also lead to smoothing of the measured  $g$ -factor profile which is not accounted for in our modeling.
- <sup>21</sup>A. Mitonneau and A. Mircea, *Solid State Commun.* **30**, 157 (1979).
- <sup>22</sup>G. M. Martin, *Appl. Phys. Lett.* **39**, 747 (1981).
- <sup>23</sup>G. Vincent, D. Bois, and A. Chantre, *J. Appl. Phys.* **53**, 3643 (1982).
- <sup>24</sup>Crooker *et al.* reported for a lower doping density of  $7.1 \times 10^{16} \text{ cm}^{-3}$  still a finite fraction of spin noise power at extrapolation to zero temperature (Ref. 32).
- <sup>25</sup>M. Oestreich *et al.*, *Phys. Rev. B* **53**, 7911 (1996).
- <sup>26</sup>M. Seck, M. Potemski, and P. Wyder, *Phys. Rev. B* **56**, 7422 (1997).
- <sup>27</sup>B. Shklovskii and A. Efros, *Electronic Properties of Doped Semiconductors*, Springer Series in Solid-State Sciences (Springer, New York, 1984).
- <sup>28</sup>J. Hübner *et al.*, *Phys. Rev. B* **79**, 193307 (2009).
- <sup>29</sup>S. O. Demokritov *et al.*, *Nature (London)* **443**, 430 (2006).
- <sup>30</sup>R. Prozorov *et al.*, *Nat. Phys.* **4**, 327 (2008).
- <sup>31</sup>K. V. Kavokin, *Semicond. Sci. Technol.* **23**, 114009 (2008).
- <sup>32</sup>S. A. Crooker, L. Cheng, and D. L. Smith, *Phys. Rev. B* **79**, 035208 (2009).